A Novel Nonlinear Stochastic-Resonance-Enhanced Acceleration Data Processing Approach

Xuyu Gao, Di He, Xin Chen, Yan Xiang, Danping Zou, Ling Pei

Shanghai Key Laboratory of Navigation and Location-based Services,
School of Sensing Science and Engineering,
School of Electronic Information and Electrical Engineering,
Shanghai Jiao Tong University – Shanghai, P.R. China - (gao_xuyu, dihe, xin.chen, yan.xiang, dpzou, ling.pei)@sjtu.edu.cn

Keywords: Stochastic Resonance (SR), Inertial Measurement Unit (IMU), Pedestrian Dead Reckoning (PDR), Localization.

Abstract

Smartphones are indispensable tools in modern social life, and they can be used for online shopping, electronic payment, gaming, and navigation. In particular, low-cost inertial measurement unit (IMU) sensors are widely integrated into smartphones, so pedestrian dead reckoning (PDR) positioning techniques based on smartphone IMU sensors have been applied and developed. PDR positioning techniques require acceleration data for step detection, step length estimation, and step heading estimation. However, due to the cost limitations of the built-in IMU sensor in smartphones, acceleration data contains measurement noise and interference, resulting in poor consistency in acceleration peak detection and the generation of false peaks, which is not conducive to step detection and accurate step length estimation. Therefore, this paper proposes a stochastic resonance (SR) enhancement method for smartphone IMU acceleration data. The SR-enhanced acceleration data has better peak consistency and is conducive to step detection. Finally, the algorithm is evaluated using actual measurement data collected from a smartphone. The results show that the SR-enhanced acceleration data has excellent peak consistency and higher step detection accuracy.

1. Introduction

Location-based services (LBS) can provide location information for people, vehicles, and objects. LBS has a wide range of applications, including route planning, autonomous driving, and disaster relief. Global navigation satellite systems (GNSS) are the most successful and widely used technology for implementing LBS and can provide LBS worldwide. The best-known GNSS systems are GPS, BeiDou, GLONASS, and Galileo. In open-sky environments, GNSS positioning accuracy can reach the meter level (Gao and Groves, 2018), which can meet the positioning needs of many fields. However, in the shade of trees, urban canyons, and indoor environments, the propagation path between the satellite and the receiver is obstructed or completely blocked, and the GNSS positioning performance is reduced or completely disabled. Therefore, achieving reliable positioning in indoor environments where GNSS signals are unavailable is an important research focus.

Many technologies have been developed and utilized for indoor positioning, including WiFi (Feng et al., 2023, Ding et al., 2022), Bluetooth (Zhuang et al., 2022, Guo et al., 2023), Ultra-wideband (UWB) (Chiasson et al., 2023, Cerro et al., 2022), and cellular systems (Chen et al., 2022, Gao et al., 2022). A common feature of these technologies is installing anchor nodes at fixed locations to observe signals between the anchor nodes and the user equipment (UE). These observations, which include time of arrival (TOA), direction of arrival (DOA), angle of arrival (AOA), and received signal strength indicator (RSSI), are processed to achieve positioning. Therefore, the above positioning method is very effective in an environment such as factories, where anchor nodes can be installed, and the UE is cooperative. However, in some indoor scenarios, we are not allowed to install anchor nodes in advance, and the functions of the UE are limited, so these methods cannot be applied.

Pedestrian dead reckoning (PDR) positioning technology uses data from an inertial measurement unit (IMU) for dead reckoning and does not rely on external signal exchange, and can be applied in indoor environments where anchor nodes are not installed. Therefore, PDR positioning technology has been extensively studied, and its implementation forms are also very diverse. On the one hand, some studies have installed IMUs in different parts of the human body to achieve PDR, such as foot-mounted IMU PDR (Ali et al., 2021, Cho and Park, 2019), waist-worn IMU PDR (Goyal et al., 2011), helmet-mount IMU PDR (Sadruddin et al., 2020), etc. On the other hand, thanks to the development of integrated circuit technology, IMUs are embedded in smartphones, and smartphones are increasingly becoming necessary. Therefore, research on PDR technology based on the IMU in smartphones has significant practical application value. For example, some studies focus on using smartphone IMU alone to achieve PDR (Kang and Han, 2015, Poulose et al., 2019). Other research focuses on combining PDR technology with different technologies, such as PDR/GNSS (Jiang et al., 2022), Wi-Fi Round Trip Time (Wi-Fi RTT) and PDR (Liu et al., 2021), Bluetooth low energy (BLE) and PDR (Kong et al., 2023), PDR/UWB (Guo et al., 2020) and so on. In addition, readers can find concluding reviews on PDR by (Wu et al., 2019).

In PDR positioning, step detection, step length estimation, and step heading estimation are the three most crucial steps (Díez et al., 2018), and accelerometer data is used for step detection and step length estimation. Step heading estimation is based on the orientation measurement of the IMU. Based on the current step point, position estimation is achieved based on the step length and heading. Therefore, step detection is the foundation of PDR, as it determines the precise moment for position updates, and incorrect step detection can result in an offset of the estimated position (Ho et al., 2016). There is much literature on step detection using smartphone IMU. For example, Wang, A. et al. implemented filtering and differential processing of smartphone acceleration data and improved the step size estimation algorithm (Wang et al., 2019). Yao, Y. et al. based on dynamic time warping (DTW), integrated peak prediction and zero-crossing detection to implement step detection, and verified the accuracy of the step detection method in three walking modes (Yao et al., 2020). Gu, F. et al. improve the accuracy of step detection by based on peak detection and utilizing the periodicity, similarity, and continuity of steps (Gu et al., 2017). Figures 2 (Wang et al., 2019), 5 (Yao et al., 2020), 11 (Gu et al., 2017), and 3 (Ho et al., 2016) illustrate the waveforms of the raw acceleration data. These images reveal significant inconsistencies in the peak data, which may be due to the poor performance of the smartphone IMU. Such poor performance adversely affects the accuracy of step detection. However, this issue has not been studied in depth. Therefore, this paper focuses on solving the problem of poor peak consistency of the original acceleration data from the smartphone IMU.

We proposed using stochastic resonance (SR) to pre-process the original acceleration data to obtain acceleration data with better peak consistency, which is beneficial for subsequent step detection. SR is a non-linear method that can use noise to enhance weak signals. Unlike traditional filtering ideas, SR uses the noise in the system as helpful information. It can be explained by Brownian particles converting some of the noise energy into signal energy under the influence of a non-linear potential function (Gammaitoni et al., 1998, Jiao et al., 2019). Figure 1 shows the effect of SR.

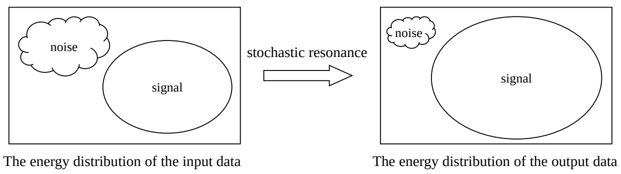

Figure 1. The signal portion of the input data is enhanced under the effect of SR.

The classical bistable model is the most common representation of SR, and it is widely used in various fields, such as mechanical fault diagnosis (Zhai et al., 2023), spectrum sensing (Li and Li, 2014), wireless channel parameter estimation (He et al., 2024) and signal detection (Chen et al., 2007). The classical bistable model deals with weak low-frequency periodic signals containing noise. When a pedestrian holds a smartphone while walking, the acceleration of IMU will show prominent periodic characteristics, and the frequency of human walking is relatively low so that these characteristics can meet the processing requirements of SR. Therefore, this paper uses SR for acceleration data processing to improve the peak uniformity of the acceleration waveform and the step detection rate.

In this paper, we proposed a method to enhance acceleration data using SR. We achieve improved peak uniformity in the original data by applying SR to process the IMU acceleration data from smartphones. With fixed detection parameters, the SR-processed acceleration data significantly improves the step detection rate compared to using the original acceleration data directly.

The rest of the paper is structured as follows. Section 2 gives a detailed description of our proposed method for SR-enhanced acceleration data. Section 3 gives test results on actual data collected from an Android smartphone. Section 4 summarizes and gives conclusions.

2. Methodology

2.1 Bistable Stochastic Resonance System

This article uses a SR system based on parameter adjustment to achieve weak signal enhancement in nonlinear systems. The Langevin equation is a typical bistable nonlinear system. The SR system can be described by the Langevin equation with double-well potential property (Fan et al., 2020):

$$\frac{dx}{dt} = -V'(x) + s(t) + N(t) \tag{1}$$

$$V(x) = -\frac{1}{2}ax^2 + \frac{1}{4}bx^4 \tag{2}$$

where $s(t)$ is the input signal of the SR system. $x(t)$ is the output signal after SR-enhanced. $N(t)$ represents the noise term, usually modeled as white Gaussian noise with a mean of zero and a variance of σ^2. $V(x)$ is the system double-well potential function. a, b is the adjustment parameter of the bistable potential well and also represents the system parameter of SR. Different SR-enhanced effects can be achieved by adjusting the values of a and b.

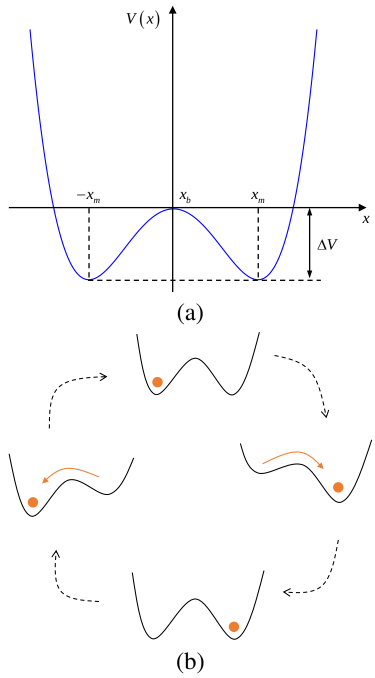

Figure 2. Schematic diagram of the double-well potential. (a) Sketch of the double-well potential, (b) switching states of the double-well potential for different parameters. (Gammaitoni et al., 1998)

As can be seen in Figure 2(a), the symmetric double-well potential reaches a minimum value at $\pm x_m$, called the stable state, a maximum value at x_b, called the unstable state, and $\Delta V = a^2/(4b)$ is called the potential barrier height (Gammaitoni et al., 1998). Figure 2(b) graphically illustrates the principle of SR. Specifically, when the system is subjected to weak periodic signals and noise, the double-well potential will deform and tilt, and the barrier height will produce periodic changes, and if the noise changes are synchronized with the periodic generation of the input signals, the phenomenon of SR is triggered and the enhancement of noise on the signal is achieved.

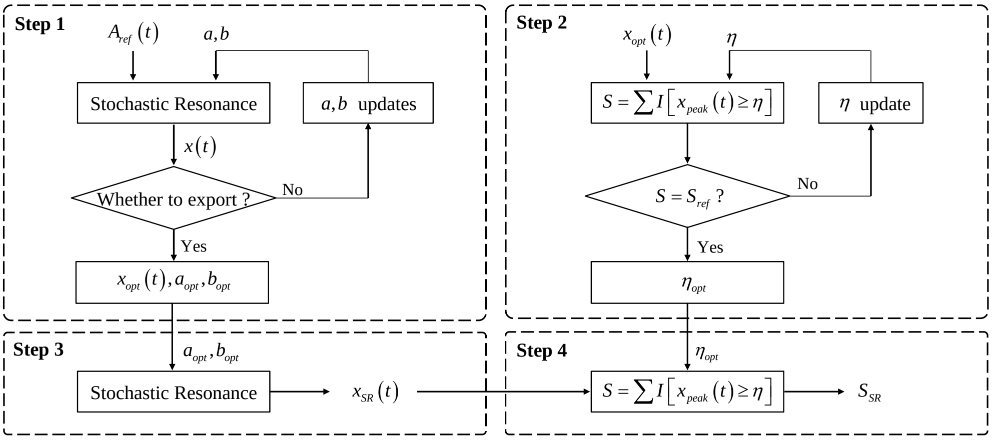

Figure 3. SR enhancement and peak step detection algorithm flow chart.

2.2 SR Enhancement and Peak Step Detection Algorithm for Acceleration Data

Step 1: Initialization of SR parameters

First, prepare a set of acceleration data $A_{ref}(t)$ with a priori known number of steps S_{true}, input $A_{ref}(t)$ into the SR system described by Equation (1), i.e., $s(t) = A_{ref}(t)$. Second, parameters a and b must be adjusted manually to obtain the SR output $x(t)$. Then, evaluate the waveform shape of $x(t)$, compare the waveform states corresponding to the different parameters a and b values, and select the optimal output waveform shape, denoted as $x_{opt}(t)$. Finally, the a and b values corresponding to $x_{opt}(t)$ are the initialized SR parameters a_{opt} and b_{opt}.

Step 2: Initialization of step detection threshold

The acceleration data $x_{opt}(t)$ after SR-enhanced using a_{opt}, b_{opt} is used to detect the step according to the following

$$S = \sum I[x_{peak}(t) \geq \eta] \tag{3}$$

where S represents the number of step detection; Σ represents the summation operation. $I[\bullet]$ is an indicator function, if the input value $\bullet$ is true, it takes 1, if $\bullet$ is false, it takes 0. $x_{peak}(t)$ denotes the peak value of the detected acceleration data $x(t)$. η represents the threshold for step detection on acceleration data.

Input $x_{opt}(t)$ into Equation (3) as $x(t)$, and continuously adjust the value of η until $S = S_{true}$. At this point, η is used as the initialized step detection threshold η_{opt}.

Step 3: Perform SR-enhanced on the acceleration data to be measured

Input the SR parameters a_{opt}, b_{opt} obtained in Step 1 and the acceleration data $A_{Ori}(t)$ to be processed into the SR system, that is, $A_{Ori}(t)$ is substituted into Equation (1) as $s(t)$, a_{opt}, b_{opt} is substituted into Equation (2) as a and b. The fourth-order Runge-Kutta method is used to solve Equation (1) (Tong et al., 2018), and the acceleration data $x_{SR}(t)$ after SR-enhanced is obtained.

Step 4: Step detection

The step detection threshold η_{opt} obtained from Step 2 is used to perform step detection on the acceleration data $x_{SR}(t)$ obtained from Step 3. Set $x(t) = x_{SR}(t)$ and $\eta = \eta_{opt}$, then substitute these into Equation (3) to perform peak step detection. Label the resulting step detection outcome as S_{SR}.

3. Experiment Evaluation

To evaluate the effectiveness of the proposed algorithm, we use actual measured IMU data from a smartphone for validation. The IMU data was acquired using an OPPO REALME RMX3366 smartphone running Android 13, with an accelerometer sampling rate of 51Hz. Volunteers handed smartphones walked at three speeds: slow, medium, fast, and then jogging. Four sets of IMU data were collected in total. The collected data underwent post-processing using Matlab 2023b.

According to the algorithm in Section 2.2, first, we select the acceleration data of medium-speed walking as $A_{ref}(t)$, and the number of steps is known to be $S_{true} = 100$. According to the requirements of Step 1, $A_{ref}(t)$ is input to SR for processing. Different outputs can be obtained after adjusting a and b, and the output with parameters $a_{opt} = 1$ and $b_{opt} = 1000$ is finally selected as the optimum output $x_{opt}(t)$. Then, enter Step 2, input $x_{opt}(t)$ into the step detector of Equation (3), continuously adjust the detection threshold η, let the output quantity S of the step detection be equal to the actual quantity S_{true}, then obtain the optimal detection threshold $\eta_{opt} = 0.8$.

Method	Parameter	η_{opt}
Original	-	0.8613
Stochastic Resonance	$a_{opt} = 1, b_{opt} = 1000.$	0.8
Butterworth Low-pass Filter	sampling frequency = 51Hz, passband frequency=2.5Hz, stopband frequency=5Hz.	0.48

Table 1. Parameters of SR and Butterworth digital LPF and optimal detection thresholds.

As a comparison, we take the original acceleration data as $x_{opt}(t)$ and input it directly into Step 2 for processing, yielding a corresponding optimal detection threshold of $\eta_{opt} = 0.8613$. Meanwhile, in order to evaluate the performance of the proposed method in compared with other methods, we designed a Butterworth digital low-pass filter (LPF) and used this LPF to process the $A_{ref}(t)$, and then the filtered acceleration data were fed into Step 2 for processing, and the optimal detection threshold $\eta_{opt} = 0.48$ was obtained. The parameters of the SR and the designed Butterworth digital LPF are summarized in Table 1, along with the optimal detection thresholds corresponding to the three methods.

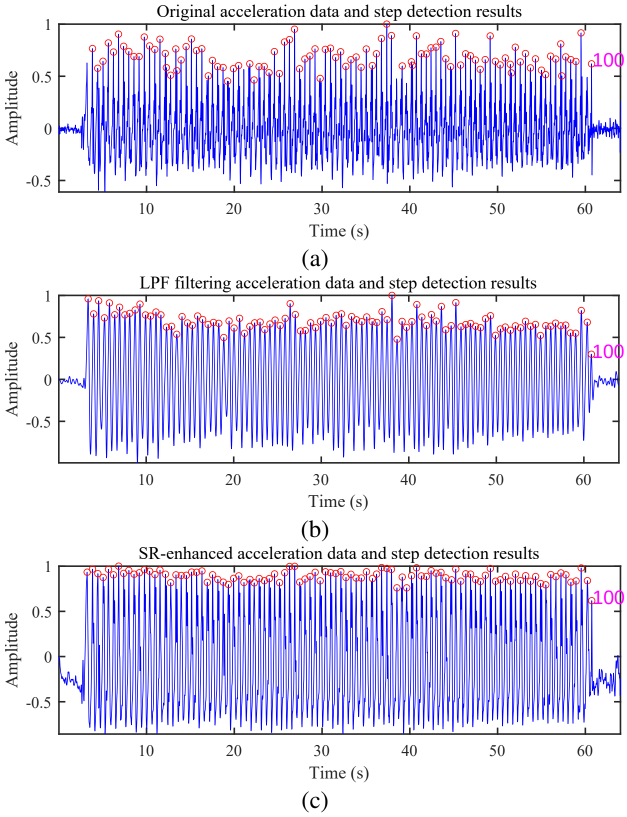

Figure 4. Step detection results for the priori acceleration data $A_{ref}(t)$. (a) Original, (b) LPF filtering, (c) SR-enhanced.

Figure 4 shows the acceleration data waveforms corresponding to the three methods, as well as the step detection results for $A_{ref}(t)$, which are obtained by using the parameters in Table 1. In Figure 4, the blue lines indicate the acceleration data, the red circle represents the detected step point, and the magenta numbers indicate the total number of detected steps. It should be noted that all the acceleration data in this section refer to the combined acceleration, i.e., $a_{com} = \sqrt{a_x^2 + a_y^2 + a_z^2}$, where a_x, a_y, a_z correspond to the acceleration data of X, Y, and Z axes, respectively. In addition, we have demeaned and normalized the combined acceleration. If there is no particular explanation, the acceleration data in the following text will still undergo the same processing.

Figure 5 demonstrates the results of processing the acceleration data for slow-speed walking using the parameters in Table 1. As can be seen from the figure, the number of step detections of the acceleration data processed using original, LPF, and SR are 33, 99, and 100, respectively. The actual number of steps is 100. Among the three methods, the detection result of directly using the original acceleration data is the worst. Therefore, the processing of the acceleration data using both SR and LPF gives better detection results, with SR being slightly more accurate than LPF.

The results of processing the acceleration data for fast-speed walking using the parameters in Table 1 are shown in Figure 6.

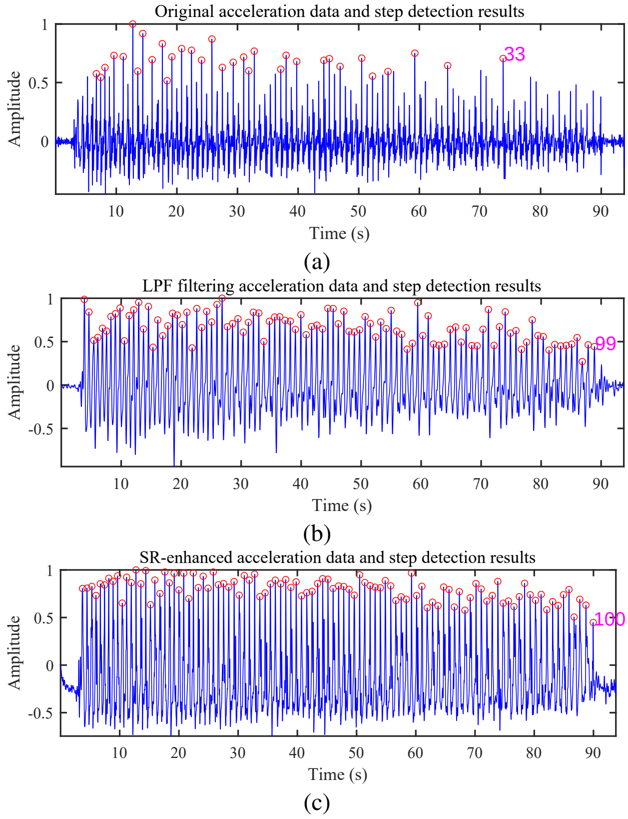

Figure 5. Step detection results after processing the acceleration data collected in slow-speed walking mode using three methods. (a) Original, (b) LPF filtering, (c) SR-enhanced.

As can be seen, the number of step detections of the acceleration data processed by the original, LPF and SR are 56, 97, and 100, respectively, and the actual number of steps is 100. The accuracy of acceleration data processing using LPF and SR is improved by 41% and 44%, respectively. It can be seen that there are three missed detections in the detection results of the LPF-processed acceleration data, resulting in a decrease of 3 in the total number of steps. In contrast, there are three false detections in the detection results of the SR-enhanced acceleration data, but the total number of paces was correct.

In order to test the robustness of the algorithm in different motion states of pedestrians, we processed the collected IMU data in the jogging mode, and the results are drawn in Figure 7. On the one hand, the detection result of using the thresholds in Table 1 directly on the original acceleration data is only 5. The reason for this result is that the IMU data produces a burr around the 40s, compared to the other moments of the acceleration data with low amplitude, which leads to poor results of the uniform threshold detection. On the other hand, the detection result using LPF is 98, and it can be seen that three relatively small peaks are not detected. Although LPF can filter out some of the burrs, the contribution of LPF to the improvement is relatively small due to the significant differences in the peaks of the acceleration waveforms. In contrast, the SR-processed acceleration data detected all the peak points with a detection rate of 100%, this is because the SR-processed data not only have a specific filtering effect on the burr filtering effect but also improves the problem of inconsistent acceleration waveform peaks to a certain extent.

From Figures 5, 6,and 7 after verifying the measured data under different pedestrian movement rates, the SR-processed accel-

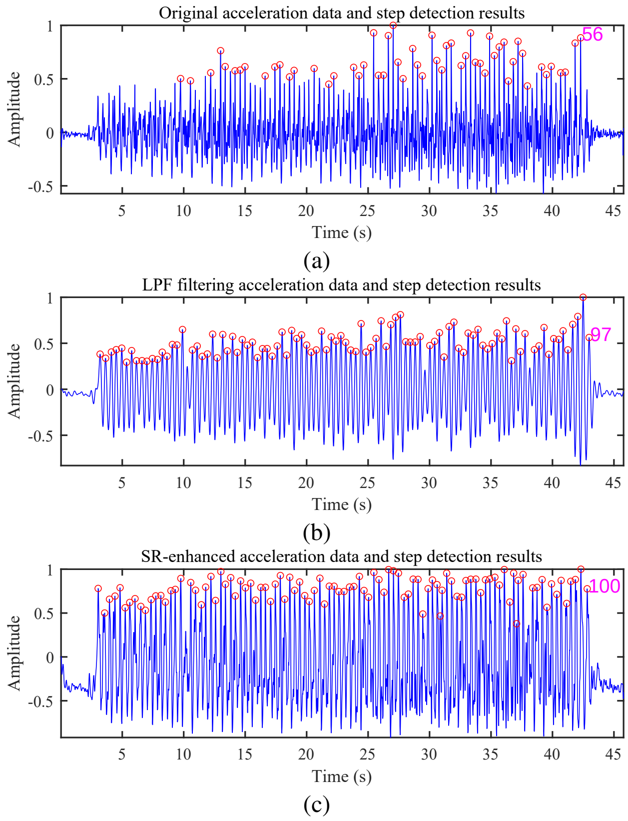

Figure 6. Step detection results after processing the acceleration data collected in fast-speed walking mode using three methods. (a) Original, (b) LPF filtering, (c) SR-enhanced.

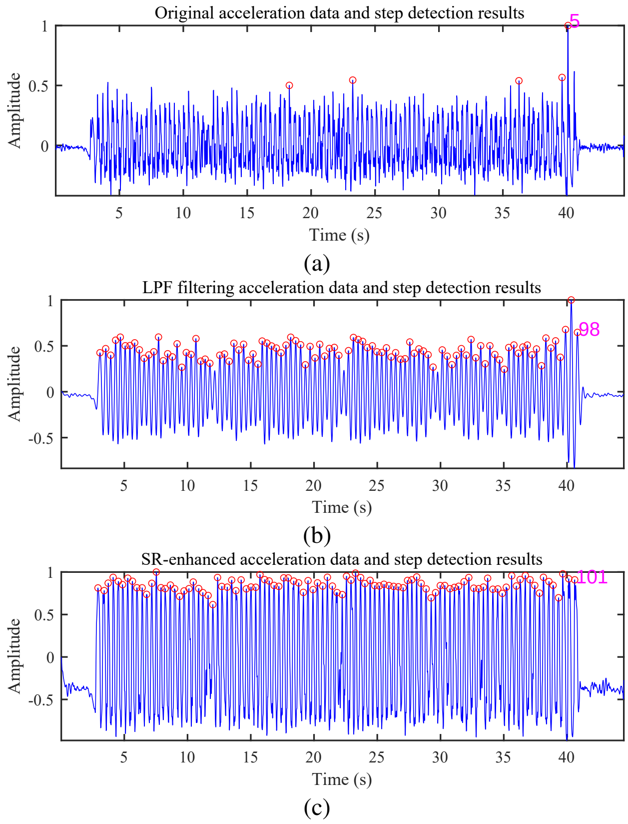

Figure 7. Step detection results after processing the acceleration data collected in jogging mode using three methods. (a) Original, (b) LPF filtering, (c) SR-enhanced.

eration data for step detection proposed in this paper achieves 100% detection probability. The proposed algorithm is more robust than directly using the original acceleration data and LPF-filtered data for step detection. At the same time, the acceleration data after SR-enhanced has better peak consistency.

4. Conclusions

This paper addresses the problem of poor peak consistency of the acceleration data from the cost-limited IMU in smartphones, which is not conducive to step detection. A method for SR-enhanced acceleration data is proposed. The processing results of the measured data show that the SR-enhanced smartphone acceleration data have better peak uniformity. Under the verification of several sets of acceleration data of pedestrians with different walking speeds, a peak step detection method with a single threshold was used to detect the original, processed by Butterworth digital LPF, and SR-enhanced acceleration data. The results show that our proposed method has a higher step detection rate, which fully demonstrates the effectiveness and robustness of the present algorithm.

However, the proposed SR-enhanced acceleration method has some drawbacks, i.e., acquiring the system parameters relies on processing a priori data set. Fortunately, the same SR system parameters can be used to process acceleration data in multiple motion modes for a particular smartphone.

5. Acknowledgements

This research work is supported by the National Natural Science Foundation of China under Grant Nos. 62231010 and 61971278, and the Shenzhen Science and Technology Innovation Commission Undertaking Major National Science and Technology Project under Grant No. CJGJZD20230724092859004.

References

Ali, R., Liu, R., Nayyar, A., Qureshi, B., Cao, Z., 2021. Tightly Coupling Fusion of UWB Ranging and IMU Pedestrian Dead Reckoning for Indoor Localization. *IEEE Access*, 9, 164206-164222.

Cerro, G., Ferrigno, L., Laracca, M., Miele, G., Milano, F., Pingerna, V., 2022. UWB-Based Indoor Localization: How to Optimally Design the Operating Setup? *IEEE Transactions on Instrumentation and Measurement*, 71, 1-12.

Chen, H., Varshney, P. K., Kay, S. M., Michels, J. H., 2007. Theory of the Stochastic Resonance Effect in Signal Detection: Part I—Fixed Detectors. *IEEE Transactions on Signal Processing*, 55(7), 3172-3184.

Chen, L., Zhou, X., Chen, F., Yang, L.-L., Chen, R., 2022. Carrier Phase Ranging for Indoor Positioning With 5G NR Signals. *IEEE Internet of Things Journal*, 9(13), 10908-10919.

Chiasson, D., Lin, Y., Kok, M., Shull, P. B., 2023. Asynchronous Hyperbolic UWB Source-Localization and Self-Localization for Indoor Tracking and Navigation. *IEEE Internet of Things Journal*, 10(13), 11655-11668.

Cho, S. Y., Park, C. G., 2019. Threshold-less zero-velocity detection algorithm for pedestrian dead reckoning. *2019 European Navigation Conference (ENC)*, 1–5.

Ding, J., Wang, Y., Si, H., Gao, S., Xing, J., 2022. Three-Dimensional Indoor Localization and Tracking for Mobile Target Based on WiFi Sensing. *IEEE Internet of Things Journal*, 9(21), 21687-21701.

Díez, L. E., Bahillo, A., Otegui, J., Otim, T., 2018. Step Length Estimation Methods Based on Inertial Sensors: A Review. *IEEE Sensors Journal*, 18(17), 6908-6926.

Fan, X., Bai, P., Liang, X., Zhang, J., Liu, B., 2020. Detection Algorithm of BPSK Signal of Parameter-Adjusted Bistable Stochastic Resonance Model Based on Scale Change. *IEEE Access*, 8, 97643-97657.

Feng, X., Nguyen, K. A., Luo, Z., 2023. A dynamic model switching algorithm for wifi fingerprinting indoor positioning. *2023 13th International Conference on Indoor Positioning and Indoor Navigation (IPIN)*, 1–6.

Gammaitoni, L., Hänggi, P., Jung, P., Marchesoni, F., 1998. Stochastic resonance. *Rev. Mod. Phys.*, 70, 223–287. https://link.aps.org/doi/10.1103/RevModPhys.70.223.

Gao, H., Groves, P. D., 2018. Environmental Context Detection for Adaptive Navigation using GNSS Measurements from a Smartphone. *NAVIGATION*, 65(1), 99-116. https://onlinelibrary.wiley.com/doi/abs/10.1002/navi.221.

Gao, K., Wang, H., Lv, H., Liu, W., 2022. Toward 5G NR High-Precision Indoor Positioning via Channel Frequency Response: A New Paradigm and Dataset Generation Method. *IEEE Journal on Selected Areas in Communications*, 40(7), 2233-2247.

Goyal, P., Ribeiro, V. J., Saran, H., Kumar, A., 2011. Strap-down pedestrian dead-reckoning system. *2011 International Conference on Indoor Positioning and Indoor Navigation*, 1–7.

Gu, F., Khoshelham, K., Shang, J., Yu, F., Wei, Z., 2017. Robust and Accurate Smartphone-Based Step Counting for Indoor Localization. *IEEE Sensors Journal*, 17(11), 3453-3460.

Guo, G., Chen, R., Yan, K., Li, P., Yuan, L., Chen, L., 2023. Multichannel and Multi-RSS Based BLE Range Estimation for Indoor Tracking of Commercial Smartphones. *IEEE Sensors Journal*, 23(24), 30728-30738.

Guo, S., Zhang, Y., Gui, X., Han, L., 2020. An Improved PDR/UWB Integrated System for Indoor Navigation Applications. *IEEE Sensors Journal*, 20(14), 8046-8061.

He, D., Wang, P., Yu, W., 2024. Stochastic-Resonance-Networks-Enhanced Wireless Channel Parameter Estimation Approach. *IEEE Internet of Things Journal*, 11(8), 14313-14327.

Ho, N.-H., Truong, P. H., Jeong, G.-M., 2016. Step-Detection and Adaptive Step-Length Estimation for Pedestrian Dead-Reckoning at Various Walking Speeds Using a Smartphone. *Sensors*, 16(9). https://www.mdpi.com/1424-8220/16/9/1423.

Jiang, C., Chen, Y., Chen, C., Jia, J., Sun, H., Wang, T., Hyyppa, J., 2022. Implementation and performance analysis of the PDR/GNSS integration on a smartphone. *GPS Solutions*, 26(3), 81. https://doi.org/10.1007/s10291-022-01260-0.

Jiao, S., Lei, S., Jiang, W., Zhang, Q., Huang, W., 2019. A Novel Type of Stochastic Resonance Potential Well Model and Its Application. *IEEE Access*, 7, 160191-160202.

Kang, W., Han, Y., 2015. SmartPDR: Smartphone-Based Pedestrian Dead Reckoning for Indoor Localization. *IEEE Sensors Journal*, 15(5), 2906-2916.

Kong, X., Wu, C., You, Y., Yuan, Y., 2023. Hybrid Indoor Positioning Method of BLE and PDR Based on Adaptive Feedback EKF With Low BLE Deployment Density. *IEEE Transactions on Instrumentation and Measurement*, 72, 1-12.

Li, Q., Li, Z., 2014. A Novel Sequential Spectrum Sensing Method in Cognitive Radio Using Suprathreshold Stochastic Resonance. *IEEE Transactions on Vehicular Technology*, 63(4), 1717-1725.

Liu, X., Zhou, B., Huang, P., Xue, W., Li, Q., Zhu, J., Qiu, L., 2021. Kalman Filter-Based Data Fusion of Wi-Fi RTT and PDR for Indoor Localization. *IEEE Sensors Journal*, 21(6), 8479-8490.

Poulose, A., Eyobu, O. S., Han, D. S., 2019. An Indoor Position-Estimation Algorithm Using Smartphone IMU Sensor Data. *IEEE Access*, 7, 11165-11177.

Sadruddin, H., Mahmoud, A., Atia, M. M., 2020. Enhancing body-mounted lidar slam using an imu-based pedestrian dead reckoning (pdr) model. *2020 IEEE 63rd International Midwest Symposium on Circuits and Systems (MWSCAS)*, 901–904.

Tong, L., Li, X., Hu, J., Ren, L., 2018. A PSO Optimization Scale-Transformation Stochastic-Resonance Algorithm With Stability Mutation Operator. *IEEE Access*, 6, 1167-1176.

Wang, A., Ou, X., Wang, B., 2019. Improved step detection and step length estimation based on pedestrian dead reckoning. *2019 IEEE 6th International Symposium on Electromagnetic Compatibility (ISEMC)*, 1–4.

Wu, Y., Zhu, H.-B., Du, Q.-X., Tang, S.-M., 2019. A Survey of the Research Status of Pedestrian Dead Reckoning Systems Based on Inertial Sensors. *International Journal of Automation and Computing*, 16(1), 65-83. https://doi.org/10.1007/s11633-018-1150-y.

Yao, Y., Pan, L., Fen, W., Xu, X., Liang, X., Xu, X., 2020. A Robust Step Detection and Stride Length Estimation for Pedestrian Dead Reckoning Using a Smartphone. *IEEE Sensors Journal*, 20(17), 9685-9697.

Zhai, Y., Fu, Y., Kang, Y., 2023. Incipient Bearing Fault Diagnosis Based on the Two-State Theory for Stochastic Resonance Systems. *IEEE Transactions on Instrumentation and Measurement*, 72, 1-11.

Zhuang, Y., Zhang, C., Huai, J., Li, Y., Chen, L., Chen, R., 2022. Bluetooth Localization Technology: Principles, Applications, and Future Trends. *IEEE Internet of Things Journal*, 9(23), 23506-23524.